

Signal Based Features with Applications to Ship Recognition in FLIR Imagery

Steve Allen^{1,2}

¹Lockheed Martin Canada,

6111 Royalmount ave, Montréal QC, H4P 1K6

²Centre de Recherches Mathématiques, Université de Montréal,

C.P. 6128 Succ. Centre-ville, Montréal QC, H3C 3J7

allen@CRM.UMontreal.CA

Abstract – *In this work, we present a new approach for ship recognition in FLIR imagery. Our algorithm is based on two kinds of features: shape features and signal features. For these last features, we accord different weights to the different pixels in the pattern, making them more robust, than shape features, with respect to the segmentation efficiency. To achieve the recognition process, we calculate the direction of principal moment axis and extract the intensity distribution along that axis. Then we use a binary tree classifier to classify a given ship. To evaluate the efficiency of our algorithm, we use the false acceptance rate. We give this rate as function of the size of the ship (function of the distance of the ship). We show that over a large distance, our algorithm gives a very low false acceptance rate.*

Keywords: Pattern recognition, Features selection, Tree classifier, Infrared imagery.

1 Introduction

In image recognition investigation, one has to pick up some features which are quite similar for each object belonging to a same class but which enable one to characterize in a distinct way every classes. In this order, features have to be translation, rotation and scaling invariant. So this is a difficult task to find features which on one hand are almost invariant for ships belonging to a same class and which on the other hand enable an accurate identification of class memberships.

Since the work by Hu [1], who proposed a set of

Euclidean invariable features, many authors have focused on the development of a classification process to build an accurate recognition algorithm. In the particular case of ship recognition, Park et Sklansky [2] has developed an automated design of linear tree classifiers. As features, they used seven invariant moments given by Hu. But, as they have denoted, these moments deliver information of primarily the global shape of the object and represent poorly the details of the object. So, they have added to these moments four parameters extracted by fitting an autoregressive model to the one-dimensional sequence of the projected image along the horizontal axis. More recently, Gouaillier and Gagnon [3] as developed an algorithm for ship recognition in SAR imagery. They have exploited the fact that in SAR imagery, the intensity gives a measure of the radar scattering rate. To do civil/military ship classification they have used the spatial distribution along nine sections of the ship target. They have completed the target identification by using a modular approach consisting of many small dedicated classifiers.

In this work, we present an algorithm for ship recognition in FLIR imagery. An important feature of FLIR imagery is to give a measure of heat distribution along the ship armour. This heat distribution gives information about engine position and about the diffusion of heat along the ship. So combining the heat distribution with shape features we build a new algorithm for ship classification. Moreover, in FLIR imagery, the segmentation of the coldest part of the target might be difficult. The fact that we attribute higher weight to the warmer part make the features, and so the classification process, robust against target segmentation accuracy. So, our work is closely re-

lated to the previous work by Gouaillier and Gagnon [3] but with a deeper focus on feature selection.

The paper is divided as follows. In the next section, we describe how we achieve translation and rotation invariance of targets. In the third, we give a description of the way we extract scaling invariant signal based features from the translation and rotation invariant patterns. Then we present a classification process based on those features. One can find results on FLIR imagery in the last section of the paper. We give the confusion matrix. Using this information, it becomes possible to use the present algorithm as a module in a fusion system which can provide a list of the most probable target identifications.

2 Pattern invariance

To identify a ship using some features, we have to be sure that the chosen features are invariant under three transformations of the given pattern: translation, rotation (in plane), scaling. There is two ways to achieve this purpose: inverting the transformations of the pattern such that it is always observed under the same *point de vue*, or choosing features which are invariant under the given transformations. For the invariance under scaling we choose the latter solution while for rotation and translation we choose the farther solution.

The weakness about choosing invariant features comes from the fact that completely invariant features contain only information on the global shape of a given ship. So they are not very useful in a recognition procedure. As we will see, “inverting” the transformation of the pattern enables one to choose features representing the details in the ship’s characteristics.

In this section, we will describe the way we make the pattern invariant under translation and under rotation. We simply have to identify a particular point and a particular axis that characterize the given ship.

As specific point, we choose the centroid position. However, the segmentation of the coldest part of the ship is quite unstable, so we attribute a weight to each point proportional to their gray level values. Let I_l be the gray level of the pixel labelled l , where $l \in [1, N_{\text{pix}}]$ with N_{pix} the number of pixels in the

pattern. The centroid position, (\bar{x}, \bar{y}) , is given by

$$\bar{x} = \sum_{l=1}^{N_{\text{pix}}} x_l p(I_l) \quad (1)$$

$$\bar{y} = \sum_{l=1}^{N_{\text{pix}}} y_l p(I_l) \quad (2)$$

The weight p is normalize to one. As mentioned, we choose it to be proportional to the gray level: $p(I_l) = a + bI_l$ where a and b are two constants and b is positive. Typically, we will choose those constants such that the weight corresponding to a given level, $I = c$, is zero: $p(c) = 0$. Then we have

$$p(I) = \frac{I - c}{\sum_l (I_l - c)} \quad (3)$$

Having computed the centroid position, we can translate the ship such that the centroid position corresponds to the origin in the (x, y) plane. Now, the translated pattern can be used to compute a particular axis direction in order to make it invariant under rotation. For this purpose, we attribute the same weight to every pixel forming the pattern. So, if the warmest part of the ship is located at one extremity of the ship, the centroid position will be close to that extremity and the ship will be very unsymmetric with regard to the centroid point. In such cases, it will be very easy to identify a dominant axis and to have a very stable expression for the direction of that axis. No matter the centroid position, we compute the principal moment axis direction, θ , according to the following expression [4]:

$$\theta = \tan^{-1} \left(\frac{M_{xx-yy} + \sqrt{M_{xx-yy}^2 + M_{xy}^2}}{M_{xy}} \right) \quad (4)$$

where

$$M_{xx-yy} = \frac{1}{N_{\text{pix}}} \sum_l [(x_l - \bar{x})^2 - (y_l - \bar{y})^2] \quad (5)$$

$$M_{xy} = \frac{2}{N_{\text{pix}}} \sum_l (x_l - \bar{x})(y_l - \bar{y}) \quad (6)$$

In the next figure, fig. 1, we show some examples which demonstrate the ability of our algorithm to make the ship invariant under translation and rotation. The images on the left hand side show raw data while the images on the right hand side are the corresponding images after segmentation and after translation and rotation of the pattern. Here, we

translate the patterns such that the centroid points correspond to the middle pixels of the images. Segmentations have been achieved by using a thresholding approach.

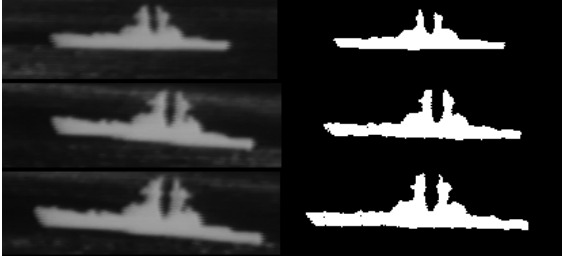


Figure 1: Segmentation and invariance of ships in FLIR imagery

3 Feature Selection

There is three principal classes of features: statistical features, structural features (also called parametrization features) and spectral features [5]. In our approach, our features are partly structural in the way that knowing that we are dealing with oblong objects, we divide the objects in sections and measure features for each section. So the set of features might be considered as a form of parametrization of the object. That's why we characterize features by the term structural. Moreover, this parametrization is well defined by the fact that we have identified a characteristic axis in the pattern. We use this axis in order to identify the upper (above the axis) and the lower part (below the axis) of a given ship. In addition to their structural character, our features are, in a first sight, statistical features.

In the case of statistical features, Hu [1] has derived moment functions invariant under translation, rotation and scaling, f_j . These functions are built with the second and third order moments given by:

$$\mu_{nm} = \frac{1}{N} \sum_l (x_l - \bar{x})^n (y_l - \bar{y})^m \quad (7)$$

where \bar{x} and \bar{y} are the mean positions along the \hat{x} and \hat{y} axes, respectively, and N is the total number of points in the sum. The order of a given moment is given by $n + m$. The fact that the moment functions, $f_j(\mu)$, are invariant under rotation involves that they contain a low amount of information about details in the shape of the pattern. So these functions are not very useful for ship recognition. That's the reason why we choose to make the pattern invariant under

rotation. This approach is quite similar to the idea of Park and Sklansky [2] who proposed to apply a projection of a ship image onto the horizontal axis.

To take a look at the intensity distribution, we divide the ship along the length in N_{sp} subparts. We denote each subpart by the set of pixels belonging to the corresponding domain S_i with $i \in [1, N_{sp}]$. Taking in account the intensity weighting, we define new moments calculate over every subpart of the ship:

$$\nu_{nm}^i = \sum_{l \in S_i} |x_l - \bar{x}_i|^n |y_l - \bar{y}|^m p(I_l) \quad (8)$$

where the sum is over all pixels belonging to the corresponding subpart. The coordinates chosen as reference, (\bar{x}_i, \bar{y}) are given by the central position along the length, $\bar{x}_i = (\max(x) + \min(x))/2$ where x belong to S_i , and the mean position in height, eq. (2). So, computing the moments up to order r , one obtains $\frac{1}{2}(r+1)(r+2)N_{sp}$ distinct features.

The last difficulty to avoid is to ensure one that the features we build are invariant under scaling and are not too much sensitive to the observation conditions. The most important barrier to achieve this purpose resides on the fact that our features depend on the gray level distribution through the weighting, eq. (3). In an ideal case we can determine the intensity dependance on the scaling ($I \propto A$, proportional to the area of the pattern). However, the data can be far from the ideal case, the intensity being largely dependant on the observation conditions. An approximate scaling independance can be reached by considering only the ratio of the moments with respect to the mean moment over every subparts of the ship. So, considering the last example of N_{sp} subparts with r moments, one obtains $\frac{1}{2}(r+1)(r+2)(N_{sp}-1)$ scaling independant features.

For the application to ship recognition, we retain only the intensity distribution, ν_{00}^i , so we have $N_{sp}-1$ independant features ($r=0$). As one can see in the next section, these features achieved a partial classification of the ship. To complete it, we add shape moments. The distinctive features of a given ship belong to the upper part of it. So, we will restrict the moments to that part and we will consider the mean height of every subpart (see eq. (7)):

$$\mu_{01}^i = \frac{1}{L} \frac{1}{N_i^+} \sum_{l \in S_i^+} (y_l - \bar{y}) \quad (9)$$

where the sums are restricted to the parts above the moment axis, $y_l > \bar{y}$, given by S_i^+ and N_i^+ represents

the number of pixels in the corresponding domain. We divide by the total length of the ship, L , in order to have scaling independent features. With those additional features, one is left with $2N_{sp} - 1$ independent features.

The number of subparts, N_{sp} is limited by the smallest length we want to be able to consider (typically $N_{sp} \simeq 7 - 9$). So, typically, we are left with 13 to 17 invariant features.

4 Classification

The classification process used is a binary tree classifier. A given ship must belong to one of the classes given in table 1. For any classes, a ship can be observed under two distinct out-of-plane angles: 30° or 90° .

In figure 2, we illustrate the tree classifier built by a training process over fifty ship images. To achieve the classification, the tree do not use directly the features measured previously. But, instead, new variables which are given by a combination of these features. Roughly speaking, at the first node we use a measure of the relative importance of the intensity at the end of the ship with respect to the intensity of the central part. As one can see, most of the military ships belong to the types of ship with a dominant central part (right branch). After that node, the *C-F* and the *CONT* can be identified by the fact that the stern is much higher than the bow. Distinction of both comes from the presence of higher structure in

| Classes | Types of ship |
|---------|-------------------------------|
| AOR | Auxiliary Oil Replenishment |
| C-F | Civilian Freighter |
| CGN | Cruiser |
| CONT | Container |
| DD | Destroyer |
| DDG | Destroyer with Guided Missile |
| FF | Frigate |
| LST | Landing Assault Tanker |

Table 1: Ship classes

the central part of the *C-F*. On the other side, our algorithm identifies *LST* from *AOR* by the presence of a long flat extremity in the farther class.

On the right branch, only the intensity distribution is used to complete the classification process. *DDG* and *FF* are characterized by the presence of a bump in the intensity distribution at midpath between the central part and the end. Then the distinction between *DDG* and *FF* is done using the fact that in the *FF* the central part is highly dominant in the intensity distribution with respect to the other section. On the other side, one can very accurately distinct *DD* from *CGN* by the presence of long ends which have a very low intensity.

5 Results

In this section, we present results obtained by testing our algorithm on 240 images. As efficiency measure we have retained the false acceptance rate (FAR).

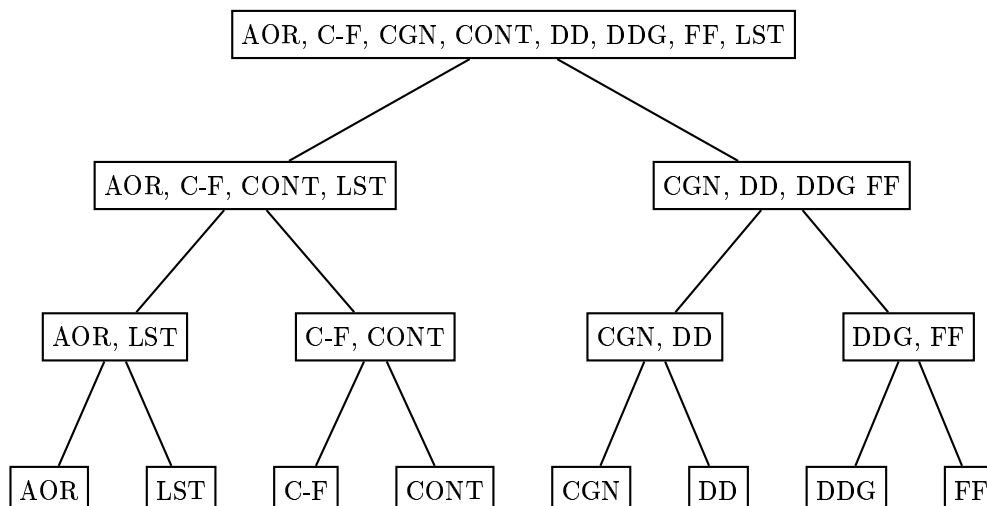


Figure 2: Tree classifier for ship recognition

| Size (pixels) | FAR |
|---------------|--------|
| > 1000 | < 2.0% |
| 500 – 1000 | 3.75% |
| 350 – 500 | 5.7% |
| 250 – 350 | 16.3% |
| 100 – 250 | 22.2% |
| < 100 | 100% |

Table 2: Ship classification false acceptance rate

Cutoffs in node conditions have been adjusted such that the classification process is as accurate as possible for the ship images at the minimum distance. In this case, it is more useful to consider the FAR as a function of ship distance. The ship distance can be evaluated by the size of the ship which is given by the number of pixels forming the pattern. We have merged the size in six different categories. In table 2, we give the FAR measured for every size categories. One has to keep in mind that a false acceptance can be due to bad segmentation, which might also cause a false estimate of the ship’s size. So the values given in the table 2 are not very accurate but serve only as an outline of the dependance of the FAR on the size of a given ship.

It follows from table 2 that our algorithm is qualified by a very accurate recognition rate for the larger ships. It has also to be noted that the most frequent false acceptances observed consist to confound *civil freighter* with *container* and confound *landing assault tank* with *frigate*. So these errors can be considered less important than the fact to confound civil with military ships.

To illustrate the confusion between classes, we give in table 3 the confusion matrix. On each row, we give the actual class belonging. The last row shows the true acceptance rate (TAR). This gives the ratio of effective appartenance to a given class with respect

to the number of times our algorithm identifies a ship to belong to the same class. On each column, we put the number of ships that was identified to belong to a given class. The last column gives the accuracy. The last row of this last column shows the overall accuracy. As pointed out previously, there is a very low rate of military/civil confusion (less than 1%).

6 Conclusion

We have shown that using intensity distribution in FLIR imagery, one can build an accurate algorithm to achieve pattern recognition. An important part of the process lie on the presence of a high moment axis which was determined using a stable expression to achieve rotation invariance. To complete the classification process we have used shape features which are less robust but give an other type of information.

The application to ship recognition as been done using the knowledge that ships are oblong object and that class membership is identified by the upper part of the ship. We have given the false acceptance rate in function of ship size to show that, if the size is not too small, our algorithm shows an almost perfect recognition success (size made up with 350 pixels and more). In goal to use this algorithm in a multisensors approach, we have given the confusion matrix. So, using a data fusion approach, one can expect to enhance the recognition process.

To improve the method presented, one should make some modifications of the segmentation step. A better segmentation may be done by using a non-universal threshold value. Another improvement can be done by using the *a priori* information that the pattern we are looking for is a ship. Then, with a cluster of ship’s signal distribution it is possible to improve all the recognition process from the segmentation to the classification step (for example see [6]).

| Class No. | AOR | C-F | CONT | LST | CGN | DD | DDG | FF | Accuracy |
|-----------|------|-----|------|-----|-----|------|-----|-----|----------|
| AOR | 12 | 0 | 0 | 0 | 0 | 0 | 0 | 0 | 100% |
| C-F | 0 | 40 | 8 | 0 | 0 | 0 | 0 | 0 | 83% |
| CONT | 0 | 3 | 33 | 0 | 0 | 0 | 0 | 0 | 93% |
| LST | 0 | 0 | 0 | 32 | 0 | 0 | 0 | 4 | 89% |
| CGN | 0 | 0 | 0 | 0 | 47 | 0 | 1 | 0 | 98% |
| DD | 0 | 0 | 0 | 0 | 2 | 22 | 0 | 0 | 93% |
| DDG | 0 | 0 | 0 | 0 | 0 | 0 | 12 | 0 | 100% |
| FF | 0 | 0 | 0 | 1 | 2 | 0 | 0 | 21 | 88% |
| TAR | 100% | 93% | 80% | 97% | 92% | 100% | 92% | 84% | 91% |

Table 3: Ship classification confusion matrix

Acknowledgments

The author wishes to thank F. Lesage and L. Gagnon for helpful discussions. This research was supported by Lockheed Martin Canada and Le Réseau de Calcul et de Modélisation Mathématique (RCM₂). FLIR images were provided by Pr. Jack Sklansky, University of California at Irvine, and taken at China Lake site, Naval Air Warfare Center.

References

- [1] M. K. Hu, *Visual pattern recognition by moment invariants*, IRE Trans. Inform. Theory, IT-8, pp. 179-187, 1962.
- [2] Y. Park and J. Sklansky, *Automated Design of Linear Tree Classifiers*, *Pattern Recognition*, Vol 23, No. 12, pp. 1393-1412, 1990.
- [3] V. Gouaillier and L. Gagnon, *Ship Silhouette Recognition Using Principal Components Analysis*, SPIE Proc. #3164, conference "Applications of Digital Image Processing XX", San Diego, 1997.
- [4] J. C. Russ, *The Image Processing Handbook*, CRC, IEEE Press, 2th edition, 1995.
- [5] R. L. Kashyap and R. Chellappa, *Stochastic Models for Closed Boundary Analysis: Representation and Reconstruction*, IEEE Trans. Inform. Theory, IT-27, pp. 627-637, 1981.
- [6] A. K. Jain, Y. Zhong and S. Lakshmanan, *Object Matching Using Deformable Templates*, IEEE Trans. PAMI, vol. 18, pp. 267-277, 1996.